Geometry of the Failure Set (System Events): Impact on the Efficiency of Simulation Methods, Adaptations of some Standard Methods

Emmanuel Ardillon
EDF-R&D, PRISME Department, Chatou, France, E-mail: emmanuel.ardillon@edf.fr
Samer Semaan
Ecole des Ponts ParisTech, Sorbonne Université, Marne-la-Vallée, France, E-mail: semaansamer6@gmail.com

ABSTRACT: Reliability assessments of penstocks performed at EDF lead to particular geometries of failure sets, that may be challenging for usual sampling methods. Two corresponding idealized geometries are investigated: a multidimensional narrow strip between two hyperplanes and two secant lines separated by a variable angle. For the narrow strip, an improvement of FORM-IS is presented in detail. It consists in building an instrumental density that enables to concentrate the sampled points in the strip. For the secant lines, line sampling, FORM-IS and subset simulation in their standard versions are investigated. First Line sampling and then FORM-IS have the most pronounced effect of the angle on the number of G-function calls N_{calls}, and the lowest N_{calls}.

1. INTRODUCTION

System events (intersection or union of events - failure or safety domains in this case) are of frequent interest in Structural Reliability, even for simple structures that are not mechanical systems. Unions of failure sets appear in the calculation of global risk of failure on a set of elements of a given population (Ardillon 2022a). Intersections can be found when taking into account temporal aspects (e.g. calculation of annual probability of failure) or information about the structural state (conditional probability of failure). These events may result in irregular shapes of the failure set, and this may impact seriously the efficiency of the standard versions of the sampling methods used for reliability assessment.

Such a situation appeared in the penstock reliability assessments recently performed at EDF, where annual, potentially conditional, failure probabilities are calculated. Simple or double intersection events had to be considered for this, resulting in two kinds of failure set geometries: narrow strips and high curvature limit state surfaces (LSS). To handle these cases, a specific method was developed: the FISTARR method based on FORM-IS (importance sampling around a relevant U* point, see (Melchers 1989)). As a complement, line sampling was also investigated and proved to be successful on this use case, provided an appropriate multiple root search algorithm was used. These methods are shortly presented in this paper.

However, for some penstock configurations these methods may converge slowly or not, and possible improvements were investigated. For doing this, idealized cases were considered, corresponding to the afore mentioned geometries: multidimensional narrow strip and high curvature LSS. The last one was represented by two intersecting lines.

This article presents some investigations performed on these two idealized cases. To our knowledge these specific failure sets have not been investigated so far in that way.

2. RELIABILITY ANALYSIS OF EDF PENSTOCKS

Steel penstocks, used for conveying water from dam to hydropower plants, are subjected to loss of thickness due to corrosion. EDF operates more than 500 penstocks (total length > 300 km).

Penstocks are pipes made of steel used to transport water under pressure from the water dam to the hydroelectric turbine. Due to thickness loss resulting from corrosion, their mechanical integrity must be justified. The usual justification relies on diagnoses involving thickness measurements and the evaluation of a deterministic margin factor (MF) which is a ratio of an allowable mechanical stress over the mechanical stress present in the pipe during operation. If this ratio is greater that one, then the penstock is considered as fit for service. The evaluation of MF depends on many variables which mainly pertain to mechanical and geometrical properties. The integrity needs to be justified for a very large panel of penstocks with different properties which justifies the need of a mechanical model. Uncertainty on some variables may affect a deterministic evaluation of the model. The conservative approach consists in evaluating MF when attributing penalized values on the uncertain variables.

To optimize MF, a general reliability approach was developed to assess the probability of failure at year N of a given penstock. Two failure modes have been identified and investigated: plastic collapse (affecting parent metal) and brittle failure (affecting welds), due to the presence of cracks appearing during the welding process. In the present paper, only the second failure mode is considered since its reliability analysis is more complex:

- the limit-state function is locally nondifferentiable and can be discontinuous;
- the annual probability of failure estimated here is a conditional probability considering that the penstock passed a hydraulic pressure test (HPT) after its production in the workshop.

By making the simplification $G_i = G_i(X)$, the conditional failure probability at year N +1 can be expressed as:

$$P_{\mathrm{f\,cond}}(MF, N) = \mathrm{Prob}((G_{N+1} < 0) \cap (G_N \geq 0) \mid (G_{HPT} > 0)) \quad (1)$$

which leads to :

$$P_{\mathrm{f\,cond}}(MF, N) = \frac{\mathrm{Prob}((G_{N+1}<0) \cap (G_N \geq 0) \cap (G_{HPT} \geq 0))}{1-\mathrm{Prob}(G_{HPT}<0)} \quad (2)$$

where G_{N+1} is the limit state function at the beginning of year N + 1, G_N is the limit state function at the beginning of year N and G_{HPT} denotes the application of the limit state function at the hydrostatic pressure with the initial thickness t_{HPT} (is the event that the penstock successfully passed the hydraulic pressure test).

More details about the mechanical and probabilistic models for penstock reliability assessments can be found in (Bryla 2020). They follow the framework given by (BS 7910 2015).

3. AN ADVANCED METHOD FOR MULTIPLE INTERSECTION EVENTS: THE FISTARR METHOD

This method has been developed specifically for penstok reliability assessments. It is based on FORM-IS: although many simulation and importance sampling techniques exist, FORM-IS (Meclchers 1989) is a popular and well-established method in the structural reliability community, which fits to the need of EDF industrial context.

Due to the particular geometrical shape of the failure set, $\{G_{N+1} < 0 \cap G_N \geq 0 \cap G_{HPT} \geq 0\}$, (an intersection of 3 events: 1 failure set intersected by 2 safe sets), the aforementioned methods, including SYS-FORM-IS, experienced convergence problems in some cases.

Indeed, as mentioned earlier the G-function is decreasing with time (for both plastic collapse and brittle fracture), which results in the following inclusion: $\{G_N(u) \leq 0\} \subset \{G_{N+1}(u) \leq 0\}$ Consequently, in the physical space as well as in the standard space, the failure set is a band intersected by another failure surface, as described in Figure 1 below. In many cases (cf. Figure 1), sampling around the individual MPFPs as with SYS-FORM-IS may not be a good strategy as it will lead to many irrelevant sampled values, falling far from the triple intersection. For such cases, the relevant MPFP to be used for sampling around can be found by adapting the usual FORM beta-point search for a single event

to multiple failure surfaces: this is the principle of Multi-constraint-FORM. In this approach, we search for $U^*_{\text{Multi-constraint}}$, such that it minimizes $\|u\|^2$ submitted to the three constraints $\{G_{N+1}(u) \leq 0\}, \{G_N(u) \geq 0\}$ and $\{G_{HPT}(u) \geq 0\}$ (cf. Figure 1).

Note that the usual algorithms suitable for a single event MPFP-search, such as Abdo-Rackwitz and Cobyla, are not appropriate in this case. Multi-constraint optimization algorithms available in the NLOPT Python Library are used instead, such as LD_AUGLAG (Augmented Lagrangian Algorithm), LD_MMA (Method of moving asymptotes), LD_SLSQP, and LN-COBYLA. LD means that the optimization is based on the local gradient. Once $U^*_{\text{Multi-constraint}}$ is found, an usual importance sampling auxiliary density is used to sample around it (Melchers 1989).

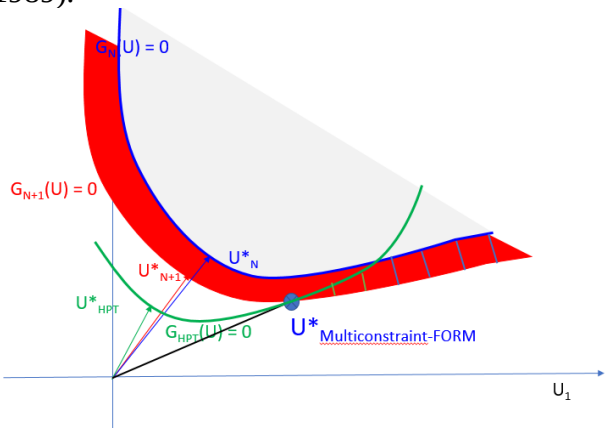

Figure 1 - Illustration of a possible failure set for penstock reliability assessments (hatched), principle of Multiconstraint-FORM used in FISTARR

Finally, to account for both situations where SYS-FORM-IS works well and those (a majority) where Multi-constraint-FORM-IS is preferable, a global sequential algorithm testing sequentially both types of algorithms is applied.

Two algorithms for SYS-FORM-IS are integrated (MPFP search with Abdo-Rackwitz or Cobyla). The four abovementioned algorithms with Multi-constraint-FORM are integrated. These algorithms are applied sequentially in a predefined order, and the method stops when an algorithm returns satisfactory results (convergence, acceptable precision - coefficient of variation - with the given computational budget). Note that the predefined order of the algorithms has been optimized regarding the convergence criterion: for that purpose a reference Design of Experiment comprising the most relevant penstock configurations (864 in total for brittle fracture and a surface-breaking crack) has been issued and the best performance algorithms have been identified (in our case LD_AUGLAG, followed by LD_MMA, and Abdo-Rackwitz).

This describes the **FISTARR** method (**F**ORM-**IS** - **T**ested **A**utomatically - **R**apid sea**R**ch). It is implemented in Persalys-Penstock (Ardillon 2022b).

4. CASE OF A NARROW STRIP

4.1. Description of the case

This case is an idealized representation of the red narrow strip of Figure 1 representing the failure set corresponding to the annual failure. It is a strip located between 2 parallel hyperplanes orthogonal to the line ($\overrightarrow{O\alpha}$), located respectively at the distance β and β+dβ from O, and thus with respective equations:

$$\sum_{i=1}^{p} \alpha_i . u_i = \beta \quad (3)$$

and

$$\sum_{i=1}^{p} \alpha_i . u_i = \beta + d\beta \quad (4)$$

The corresponding failure set is presented in Figure 2.

Its failure probability P_f is easy to compute and equals $\Phi(-\beta) - \Phi(-(\beta + d\beta))$, which can be approximated by $\phi(-\beta).d\beta$ for dβ sufficiently small, where ϕ and Φ denote the probability density function (PDF) and cumulative distribution function (CDF) of the normal standard law respectively. It should be noted that in this case, only 1 iteration (multiplied by the number of iterions needed for the search of the 2 intersections with the limit state surfaces) is necessary for the Line Sampling estimator to obtain the value of P_f. More generally, it is well known that the Line Sampling technique is well suited to limit state surfaces. For that reason, it is

proposed in the following to concentrate only on FORM-IS.

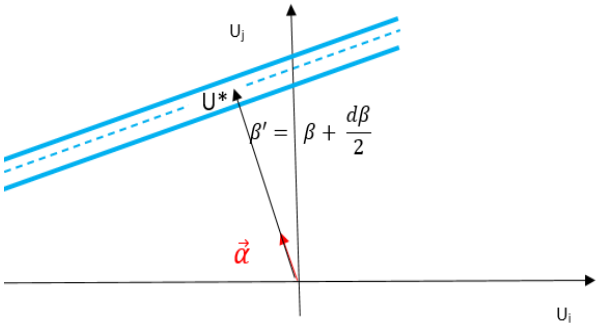

Figure 2 – Illustration of a narrow band in dimension 2

4.2. Improved FORM-IS for the narrow strip (dimension p): mathematical resolution

The idea is to build an instrumental density such that the sampled points are concentrated in the strip, or close to it. Note that a general adaptive density as proposed in (Bucher 1988) would not be relevant, since the first step would anyway require a large number of calls to get sufficiently numerous points in the narrow strip. On the contrary, a better approach is to take account of the knowledge about the failure set geometry. For this purpose, the density should be:

- Centered around the U* point, such that $\overrightarrow{OU^*} = \left(\beta + \frac{d\beta}{2}\right).\vec{\alpha}$ (cf. figure 2);
- With a standard deviation equal to $\frac{d\beta}{2}$ in the direction $\vec{\alpha}$, and "almost" equal to 1 in the directions comprised in the orthogonal hyperplan $\sum_{i=1}^{p} \alpha_i . u_i = \text{constant}$

Let us denote $\beta' = \beta + \frac{d\beta}{2}$

To build this density, the following 4 steps are proposed:

1 Identification of an i_0 index corresponding to the maximum value of $|\alpha_{i=1\ldots p}|$; it should be noted that in no structural reliability problem all the coefficients have the same sign;

2 Starting from n standard normal variables u_i, independent and identically distirbuted, the proposed new importance density consists in introducing the following variables:

a. For i ≠ i0, $u'_i = u_i + u_i^*$, with $u_i^* = \beta' . \alpha_i$ (cf. (Lemaire 2009))

b. $u'_{i0} = \frac{(\beta' + \sigma . u_{i0} - \sum_{i \neq i0}^{p} \alpha_i . u'_i)}{\alpha_{i0}}$, with for example $\sigma = \frac{d\beta}{2}$

In other words, the p-1 first variables correspond to the standard FORM-IS method, whereas the last one will be in a way that the sampled point falls in a band with standard deviation equal $\sigma = \frac{d\beta}{2}$ around the hyperplane of equation

$$\sum_{i=1}^{p} \alpha_i . u'_i = \beta + d\beta/2 \qquad (5)$$

This selection of σ is inspired from the adaptive importance sampling procedure proposed in (Bucher 1988).

3 Then, it is necessary to compute the ratio of the initial f and instrumental g densities $R(u'_1, \ldots, u'_p) = f(u'_1, \ldots, u'_p)/g(u'_1, \ldots, u'_p)$, on which is based the IS probability estimator; this calculation is detailed below;

4 Finally the estimator is as follows:

$$\widetilde{P_f} = \frac{1}{N} . \sum_{k=1}^{N} R\left(u'^{(k)}_1, \ldots, u'^{(k)}_p\right) . 1_{D_f}\left(u'^{(k)}_1, \ldots, u'^{(k)}_p\right) \qquad (6)$$

<u>Calculation of the likelihood ratio R :</u>

Various general remarks will help to perform this calculation:

- For i ≠ i0, the variables u'_i *or* u_i are independent ;
- For i = 1…p, the variables u_i are independant and the joint density f is the product of the p marginal densities ;
- For g we have to distinguish u'_{i0} from the remaining p-1 variables: we have

$$g(u'_1, \ldots, u'_p) = \prod_{i \neq i0}^{p} \varphi(u_i) . \; h(u'_{i0} | u'_{i \neq i0, i=1\ldots p}) \qquad (7)$$

where

$h(u'_{i0} | u'_{i \neq i0, i=1\ldots p})$ is the density of a normal law:

- with mean : $\frac{(\beta' - \sum_{i\neq i0}^{p} \alpha_i.u'_i)}{\alpha_{i0}}$

- with standard deviation : $\frac{\sigma}{|\alpha_{i0}|}$

The likelihood ratio R is finally the product of two ratios: one ratio R_1 concerning the $u_i \neq u_{i0}$ multiplied by a ratio involving only u_{i0}.

Calculation of R_1

It is inspired from (Lemaire 2009).

One gets:

$$R_1 = \prod_{i\#i0}^{p} \frac{\varphi(u_i+u_i^*)}{\varphi(u_i)} = \exp\left(-\beta'.\sum_{i\neq i0}^{p} \alpha_i.u_i - \frac{\beta'^2.(1-\alpha_{i0}^2)}{2}\right) \quad (8)$$

Calculation of R_2

One gets:

$$R_2 = \frac{\varphi(u'_{i0})}{h(u'_{i0}|u'_{i\,\#\,i0,i=1\ldots p})} \quad (9)$$

$$= \frac{\exp\left(-\frac{u'^2_{i0}}{2}\right)}{\frac{1}{\frac{\sigma}{|\alpha_{i0}|}}.\exp\left(-\frac{1}{2}.\left[\frac{u'_{i0} - \frac{(\beta' - \sum_{i\neq i0}^{p} \alpha_i.u'_i)}{\alpha_{i0}}}{\frac{\sigma}{\alpha_{i0}}}\right]^2\right)}$$

And finally (10):

$$R_2 = \frac{\sigma}{|\alpha_{i0}|}.\exp\left(-\frac{1}{2}\left[u'^2_{i0} - \left(\frac{\left(\sum_{i=1}^{p} \alpha_i.u'_i - \beta'\right)}{\sigma}\right)^2\right]\right)$$

Calculation of the standard deviation and variation coefficient of the estimator

It is based on the variance estimation given in (Lemaire 2009) for the standard FORM-IS estimator.

$$\widetilde{var}(\widetilde{P_{f,N}}) \quad (11)$$

$$= \frac{1}{N-1}\left[\frac{1}{N}.\sum_{k=1}^{N} R\left(u'^{(k)}_1, \ldots, u'^{(k)}_p\right)^2 . 1_{D_f}\left(u'^{(k)}_1, \ldots, u'^{(k)}_p\right) - \tilde{P}^2_{f,N}\right]$$

Note that the estimator and its coefficient of variation can be calculated iteratively.

In any case, it appears that it is not necessary to replace the bottom of the component, it is sufficient to repair some points (8 to 11).

4.3. Some results

First the following figure in dimension 2 confirms that the sampled points are concentrated around the narrow strip, as intended. It corresponds to (α_1 = -0.5; α_2 = 0.86). The target coefficient of variation cv is fixed to 0.1; 35 sampled points over 48 are in the failure set (narrow strip).

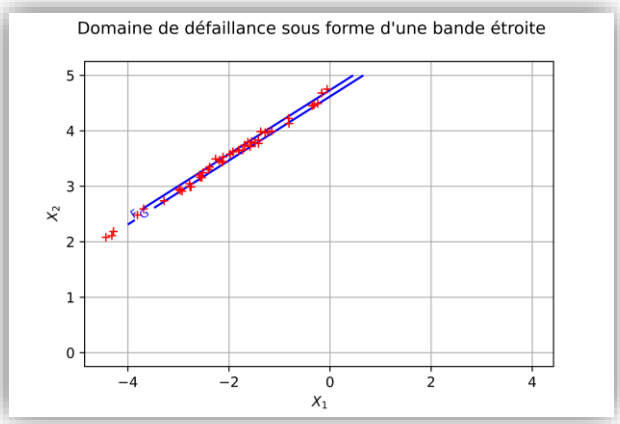

Figure 3 – Sampled points by improved FORM-IS for a narrow strip in dimension 2

The numerical results presented below are obtained for β = 4, and dβ = 10^{-1}, 10^{-2}, 10^{-3}, and 10^{-4}. The standard deviation equals dβ/2 in the direction $\vec{\alpha}$, and almost 1 in the directions located in the orthogonal hyperplane $\sum_{i=1}^{p} \alpha_i.u_i =$ constant. It is reminded that $\sum_{i=1}^{p} \alpha_i^2 = 1$. The target coefficient of variation cv is fixed to 1. Note that for the two examples, the reference probabilies are identical as they only depend on β and dβ. Moreover, these probabilities can be approximated by ϕ(-β).dβ as seen in §4.1 and consequently, they are divided by 10 if dβ is divided by 10.

Two results are given: the first one in dimension 5 and the second one in dimension 10.

$P_{f,\ ref}$ stands for the reference probability obtained with FORM. As mentioned before, the probability is (almost) proportional to the band

width dβ for dβ << 1, which is clearly confirmed by the numerical results.

N_{calls} denotes the number of calls of the G-function.

First example (p=5)

It corresponds to ($\alpha_1 = -0,25$; $\alpha_2 = 0,5$; $\alpha_3 = -0,75$; $\alpha_4 = 0,25$; $\alpha_5 = 0,25$).

Table 1: Number of limit state function calls with the improved FORM-IS for narrow strips of different widths (p=5)

dβ	*Time(s)*	$P_{f,ref}$	$\widetilde{P}_f$	*Standard deviation* ($\widetilde{P}_f$)	N_{calls}
10^{-1}	*0,0052*	*1,10 E-05*	*1,19 E-05*	*1,19E-06*	*60*
10^{-2}	*0,0018*	*1,31 E-06*	*1,43 E-06*	*1,42E-07*	*57*
10^{-3}	*0,0017*	*1,34 E-07*	*1,46 E-07*	*1,44E-08*	*57*
10^{-4}	*0,0053*	*1,34 E-08*	*1,46 E-08*	*1,44E-09*	*57*

Second example (p=10)

It corresponds to ($\alpha_1 = -0,25$; $\alpha_2 = 0$; $\alpha_3 = -0,433$; $\alpha_4 = 0,5$; $\alpha_5 = 0,25$; $\alpha_6 = 0,25$; $\alpha_7 = 0$; $\alpha_8 = 0,5$; $\alpha_9 = 0,25$; $\alpha_{10} = -0,25$)

Table 2: Number of LSF calls with the improved FORM-IS for narrow strips of different widths (p=10)

dβ	*Time (s)*	$P_{f,ref}$	$\widetilde{P}_f$	*Standard deviation* ($\widetilde{P}_f$)	N_{calls}
10^{-1}	*0,0144*	*1,10E-05*	*1,00E-05*	*1,00E-06*	*143*
10^{-2}	*0,0018*	*1,31E-06*	*1,27E-06*	*1,26E-07*	*132*
10^{-3}	*0,0017*	*1,34E-07*	*1,45E-07*	*1,44E-08*	*125*
10^{-4}	*0,0053*	*1,34E-08*	*1,29E-08*	*1,29E-09*	*132*

It can be noted that N_{calls} is almost independent from the band width dβ since the standard deviation in the direction $\vec{\alpha}$ orthogonal to the strip is directly related to dβ, whereas N_{calls} would increase significantly when dβ decreases if the standard deviation was constant, as in standard FORM-IS. Indeed, a similar study performed in dimension 2 showed the following N_{calls} for standard FORM-IS and improved FORM-IS. It can be seen that standard FORM-IS is irrelevant for narrow strips, whereas improved FORM-IS performs very well.

Table 3: Number of LSF calls with the standard and improved FORM-IS for horizontal narrow strips of different widths (p=2)

dβ	10^{-1}	10^{-2}	10^{-3}	10^{-4}
N_{calls} *(Standard FORM-IS)*	*3260*	*34775*	*302245*	*2620580*
N_{calls} *(Improved FORM-IS)*	*80*	*75*	*75*	*75*

This property is particularly interesting for low values of dβ. Moreover, N_{calls} slightly increases with the dimension p, but this may be caused by the particular values of the α_i factors.

Considering the successful performance of this improved FORM-IS for the idealized narrow strips investigated, an adapted version is being integrated to the new version of Persalys-Penstock (V1.7) under development.

5. CASE OF TWO SECANT LINES (DIMENSION 2)

The objective is to quantify the potential impact of the angle θ between the two lines. This angle represents in a certain sense the LSS curvature at the beta-point U*. Note that this notion of angle between two hyperplanes is also defined in any dimension, since it is possible to define the angle between the two vectors orthogonal to each hyperplane.

5.1. Description of the case

It is presented in figure 4 below.

The two lines intersect at U*(0, β=4)

Θ = 180° corresponds to a linear LSS. The most acute angle studied is θ = 18°, corresponding to high "curvature" and non linearity.

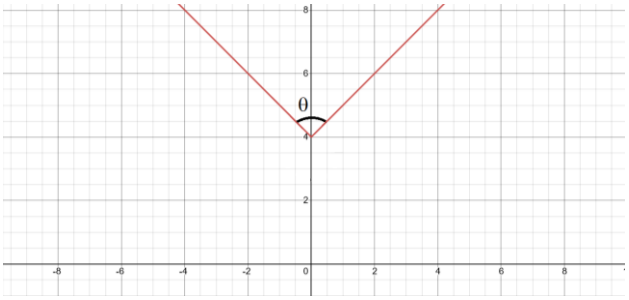

Figure 4: case of two secant lines

For this case the reference probability can be obtained by System-FORM, denoted SYS-FORM (Lemaire 2009). The simple FOR method is of course irrelevant here. The other methods compared are: Monte Carlo, FORM-IS (standard version), Subset Simulation (SS), and Line Sampling (LS). The simulation results are given for a similar precision for all methods (target cv = 10%). Two ratios R1 and R2 are defined: for each method, R1 = $N_{calls}(\theta)/N_{calls}(180°)$, and R2 = $P_f(\theta)/P_f(180°)$. For LS, it is possible in our example to find immediately the root (intersection between the line and the LSS); usually about 6 iterations may be necessary, therefore for a general evaluation of the LS performance, N_{calls}(LS) should be multiplied by 6 (Ajenjo 2022).

5.2. Some results

They are presented in Table 4 below.

All probabilities P_f are consistent with the reference value from SYS-FORM. For all methods, the ratios R2 are almost identical since they refer to the same probabilities.

For Monte Carlo, R1 and R2 are identical as expected, since cv is fixed and $cv \approx \frac{1}{\sqrt{N.P_f}}$. The increase of N_{calls} is only due to the decrease of P_f, this is not a matter of angle (curvature).

For SS, R1 increases slowly when θ decreases, but N_{calls} is high.

For LS, R1 is not relevant since it may induce erroneous conclusions regarding the performance of LS (R1 would have very high values whereas LS has the lowest N_{calls}). Contrary to MC, the increase of N_{calls} is only due to the decrease of the angle (curvature), not to the decrease of P_f. LS exhibits the most rapid convergence except for vary acute angles (high curvatures), even when multiplying N_{calls} by 6 as suggested before. For θ = 18°, LS and FORM-IS provide a similar performance (N_{calls}).

Table 4: Number of LSF calls and P_f evolution as a function of the angle θ for each method

θ (deg)	Method	N_{calls}	Pf	R1 (N_{calls})	R2 (P_f)
180	SYS-FORM	26	3,17E-05	1,00	1,00
	MC	3381144	2,96E-05	1,00	1,00
	SS	57435	3,18E-05	1,00	1,00
	FORM-IS	600	2,71E-05	1,00	1,00
	LS	1	3,17E-05		1,00
144	SYS-FORM	20	1,35E-05	0,77	2,35
	MC	7916853	1,26E-05	2,34	2,35
	SS	60465	1,39E-05	1,05	2,29
	FORM-IS	800	1,39E-05	1,33	1,95
	LS	23	1,50E-05		2,11
90	SYS-FORM	13	5,47E-06	0,50	5,80
	MC	19078585	5,24E-06	5,64	5,65
	SS	76800	6,41E-06	1,34	4,96
	FORM-IS	1905	5,43E-06	3,18	4,99
	LS	205	5,06E-06		6,26
54	SYS-FORM	7	2,87E-06	0,27	11,05
	MC	36058783	2,77E-06	10,66	10,69
	SS	94368	2,70E-06	1,64	11,78
	FORM-IS	4150	2,76E-06	6,92	9,82
	LS	390	3,06E-06		10,36
18	SYS-FORM	7	9,02E-07	0,27	35,14
	MC	119651769	8,36E-07	35,39	35,41
	SS	148380	1,04E-06	2,58	30,58
	FORM-IS	10205	8,89E-07	17,01	30,48
	LS	1750	8,68E-07		36,52

For standard FORM-IS, the increase of R1 with decrease of θ is significant, but lower than with Monte Carlo. N_{calls} remains low compared to MC and SS, but higher than for LS.

It is now necessary to investigate if this behavior originates only from the evolution of the probability or specifically from the evolution of the angle (that induces a decrease of probability). The following table gives the comparison of the evolution of N_{calls} for two cases with similar P_f: one for θ = 180° (Case 2) and one for θ = 18°.

Table 5: Compared evolution of N_{calls} for two cases with similar failure probabilities

	Case 1 β=4 (θ=180°)	***Case 2 β=5 (θ=180°)***	***Case 3 β=4 (θ=18°)***
P_f	*3,2 10^{-5}*	*2,9 10^{-7}*	*9. 10^{-7}*
SS (N_{calls})	*57435*	*139440*	*148380*
FORM-IS (N_{calls})	*600*	*765*	*10205*
LS (N_{calls})	*1*	*1*	*1750*

From this analysis the following conclusions can be drawn:

Table 6: Effect of the angle (curvature) on the method performance

Method	*Effect of the angle*
MC	*High effect only due to the evolution of the probability P_f, not specifically to the angle*
SS	*Low effect basically due to the probability, but high number of calls*
FORM-IS	*High effect basically due to the angle, low number of simulations*
LS	*High effect only due to the angle, very low number of simulations*

6. CONCLUSION

Reliability assessments of penstocks performed at EDF lead to particular geometries of failure sets, that may be challenging for usual sampling methods. Two corresponding idealized geometries have been investigated: a multidimensional narrow strip between two hyperplanes and two secant lines separated by a variable angle. For the narrow strip, an improvement of FORM-IS has presented in detail. It consists in building an instrumental density that enables to concentrate the sampled points in the strip. This development is under integration in the software dedicated to penstock reliability assessments, Persalys-Penstock. For the secant lines, line sampling, FORM-IS and subset simulation in their standard versions are investigated. First Line sampling and then FORM-IS have the most pronounced effect of the angle on the number of G-function calls N_{calls}, and the lowest N_{calls}. These developments could be useful for similar failure sets (intersection events).

7. REFERENCES

Ajenjo A., Ardillon E., Chabridon V., Cogan S., & Sadoulet-Reboul E. (2022). Info-gap robustness evaluation of a Line-sampling-based reliability assessment of penstocks. *Proceedings of the 13rd International Conference On Structural Safety and Reliability*, Shanghai, China

Ardillon E., Yang X. (2022a). Optimizing the maintenance of steel components in French nuclear power plants by a probabilistic approach, *Proceedings of the 13rd International Conference on Structural Safety and Reliability*, Shanghai, China

Ardillon E., Bryla P. & Dumas A. (2022b). Penstock reliability assessments: some results and developments, *Proceedings of the 13rd International Conference on Structural Safety and Reliability*, Shanghai, China

Baudin, M., Dutfoy, A., Iooss, B. & Popelin, A.-L. (2017). OpenTURNS: An industrial software for uncertainty quantification in simulation. In: Handbook of uncertainty quantification, R. Ghanem, D. Higdon and H. Owhadi (Eds), Springer. HAL version - Springer link

Bryla P., Ardillon E., & Dumas A. (2020). Probabilistic models for penstock integrity assessment – *Proceedings of the ESREL 2020 Conference*, Venice, Italy

BS 7910 (2015). Guide to methods for assessing the acceptability of flaws in metallic structures. British Standard Institute.

Bucher C. (1988). Adaptive sampling – an iterative fast Monte Carlo procedure – Structural Safety 5: 119-126

Lemaire M. (2009). *Structural Reliability*. Ed. by Jacky Mazars. London: ISTE Ltd., Wiley

Melchers R.E.1989. Importance sampling in structural systems. *Structural Safety* 6(1):3-10